



ARCHIVIO ISTITUZIONALE DELLA RICERCA

Alma Mater Studiorum Università di Bologna Archivio istituzionale della ricerca

Performance-based seismic design of multistory frame structures equipped with crescent-shaped brace

This is the final peer-reviewed author's accepted manuscript (postprint) of the following publication:

Published Version:

Performance-based seismic design of multistory frame structures equipped with crescent-shaped brace / Kammouh, Omar; Silvestri, Stefano; Palermo, Michele; Cimellaro, Gian Paolo*. - In: STRUCTURAL CONTROL & HEALTH MONITORING. - ISSN 1545-2255. - ELETTRONICO. - 25:2(2018), pp. e2079.1-e2079.17. [10.1002/stc.2079]

This version is available at: <https://hdl.handle.net/11585/621252> since: 2019-02-04

Published:

DOI: <http://doi.org/10.1002/stc.2079>

Terms of use:

Some rights reserved. The terms and conditions for the reuse of this version of the manuscript are specified in the publishing policy. For all terms of use and more information see the publisher's website.

(Article begins on next page)

This item was downloaded from IRIS Università di Bologna (<https://cris.unibo.it/>).
When citing, please refer to the published version.

This is the final peer-reviewed accepted manuscript of:

Kammouh, O, Silvestri, S, Palermo, M, Cimellaro, GP. Performance-based seismic design of multistory frame structures equipped with crescent-shaped brace. Struct Control Health Monit. 2018; 25:e2079.

The final published version is available online at:

<https://doi.org/10.1002/stc.2079>

Rights / License:

The terms and conditions for the reuse of this version of the manuscript are specified in the publishing policy. For all terms of use and more information see the publisher's website.

This item was downloaded from IRIS Università di Bologna (<https://cris.unibo.it/>)

When citing, please refer to the published version.

Performance-based seismic design of multi-storey frame structures equipped with Crescent-Shaped Brace

Omar Kammouh¹ | Stefano Silvestri² | Michele Palermo² | Gian Paolo Cimellaro^{1*}

¹Department of Structural, Geotechnical and Building Engineering (DISEG), Politecnico di Torino, Corso Duca degli Abruzzi 24, Turin 10129, Italy

²Department of Civil Engineering, University of Bologna, Bologna, Italy

* Corresponding author

ABSTRACT

The primary objective of the *Performance-Based Seismic Design* (PBSD) is to provide stipulated seismic performances for building structures. However, a certain degree of design freedom is needed for matching a specific seismic response. This design freedom is not obtainable by the conventional lateral resisting systems because their stiffness and strength are coupled. Here, we put emphasis on the role of the unconventional lateral resisting systems in adding more flexibility to the design. In this paper, we seek to explore the seismic design of moment resisting frame structures equipped with an innovative hysteretic device, known as *Crescent-Shaped Brace* (CSB). One conspicuous feature of this device is its distinctive geometrical configuration, which is responsible for the enhanced nonlinear force-displacement behavior exhibited by the device. A new performance-based approach for the seismic design of the CSB is proposed. The performance of the device is evaluated and its application in multi-storey shear-type structures is investigated. Two case studies were established to illustrate the design methodology. The first is a new two-storey RC structure and the second is an existing three-storey RC structure. Nonlinear time history and pushover analyses are performed to evaluate the behavior of the controlled structures. The analyses show that for each of the two case studies the acceleration-displacement capacity spectrum conforms to the performance objectives curve. This finding confirms the validity of the proposed design approach and the effectiveness of the new hysteretic device in resisting lateral forces.

Keywords: *Crescent Shaped Brace, Design method, Dynamic analysis, Performance Based Seismic Design.*

1 INTRODUCTION

Recent development in earthquake engineering has resulted in the emergence of new structural design approaches such as the Performance-Based Seismic Design (PBSD) [1]. PBSD is still deemed as a new approach even though its origin can be traced back as far as the late 20th century. The design efficiency of PBSD is the main reason behind its emergence [2]. The Performance-Based Design specifies the main objectives that should be attained by the structure and gives the standards for accepting a specified performance [3]. Today, structures are designed with the goal of achieving a predefined functionality. This is because the challenge is no longer limited to protecting human lives, but extended to minimizing damages and disruption down to reasonable levels. Nevertheless, matching a defined seismic response necessitates additional design freedom that is unable to be achieved by the traditional structural components, such as beams and columns. Here, it is necessary to emphasize the role of the unconventional lateral resisting systems in making the design more flexible and thus allowing to reach specific seismic performances.

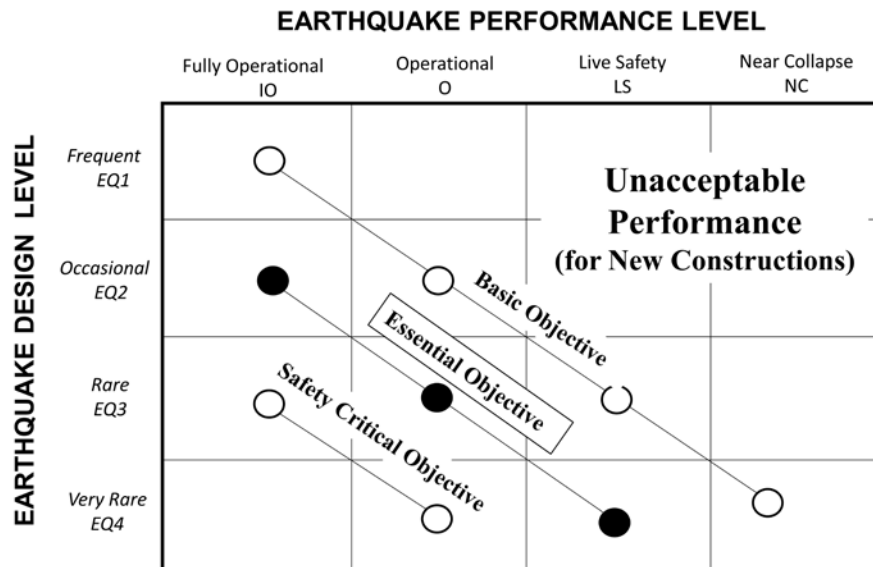
Lately, several efforts in the earthquake engineering discipline could find their ways into various advanced lateral resisting systems. These systems can provide enhanced performances to the structure under particular ground motion levels. Examples of such systems include: (a) seismic isolation systems, which disengage the superstructure from its substructure, thereby giving rise to a “conceptual separation between the horizontal and vertical resisting systems” [4]; (b) tuned mass damping systems, which are practically employed to reduce the vibration level of the structure resulted from high lateral excitations [5]; (c) active and semi-active systems, which use the actual seismic vibration to modify the mechanical properties of the structure accordingly [6]; (d) dissipative systems, which are integrated into the superstructure to reduce the damage in the structure through their energy dissipation capability [7]. Whilst the listed systems have been nicely

52 incorporated into practice and literature, none of them could completely fulfil the intended seismic
 53 objectives of structures as outlined by the PBSD.

54 In this paper, we focus on a new innovative lateral resisting device, the *Crescent Shaped*
 55 *Brace* (CSB). CSB is a hysteretic device that is grouped under the ‘energy dissipation devices’
 56 classification. The device enables the structure to have prescribed multiple seismic
 57 performance through its passive resisting capability [8]. Up to the present time, the design of multi
 58 storey buildings equipped with Crescent Shaped Braces has not been exposed to wide-ranging
 59 research. The application of the CSBs is restricted to a single case study of a steel structure in which
 60 the braces were inserted at the ground floor. The objective of that study was to obtain a controlled
 61 soft-storey response. The upper storeys were braced with conventional concentric steel diagonal
 62 braces in order to conceptually model the system as a single degree of freedom (SDOF) system [4].

63 The work presented in this study proposes a comprehensive method for the seismic design of
 64 multi storey shear-type-structures strengthened with CSB devices. In this study, the geometrical and
 65 mechanical properties of the controlled structure are assumed to be given, as in the case of existing
 66 structures; therefore, there is no control on the structure’s stiffness and strength. This implies that
 67 the CSB system is the only variable in the design. In the case of designing new structures, more
 68 design freedom is added as the properties of the structure can be chosen in accordance with the
 69 desired performance objectives. The design method proposed in the study involves: (i) sizing the
 70 CSB devices in the elastic field; (ii) verifying the behavior of the braces in the plastic field. The first
 71 part of the method is to design the braces in the elastic field with reference to a predefined
 72 performance point. Then, the post yielding behavior of the CSB is determined numerically using the
 73 FEM software ‘SeismoStruct V.7.0.6’ [9]. In the second part of the method, the post yielding
 74 behavior of the controlled system (i.e. structure equipped with the designed braces) is verified by
 75 means of nonlinear pushover and time history analyses.

76 To illustrate the procedure in all the details, the methodology has been applied to two case
 77 study structures. The controlled structures are designed to satisfy the ‘Essential Objectives’ shown in
 78 Figure 1 [1]. Non-linear pushover and time-history analyses are performed to verify the performance
 79 of the controlled system under a given seismic input. The outcome of the study proved the validity of
 80 the proposed design method and the efficiency of the hysteretic device.



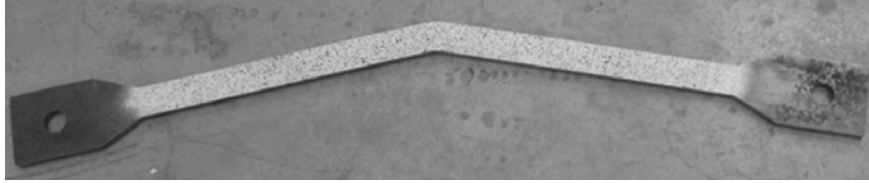
81
 82 Figure 1. Performance-based seismic design goals. Adopted from [1]

83

84 **2 THE CRESCENT SHAPED BRACES**

85 **2.1 Overview**

86 The Crescent-Shaped brace (CSB) (Figure 2) is a unique hysteretic lateral resisting device
 87 that provides additional design freedom to frame structures. Its geometrical configuration, as shown
 88 in Figure 3, permits the structure to have predefined multiple seismic performances [8]. The CSB
 89 enables the designer to have full control over the design because its yielding strength and lateral
 90 stiffness are not coupled.



91
92 Figure 2. A sample of the Crescent Shaped Brace

93
94 **2.2 Analytic model of the CSB**

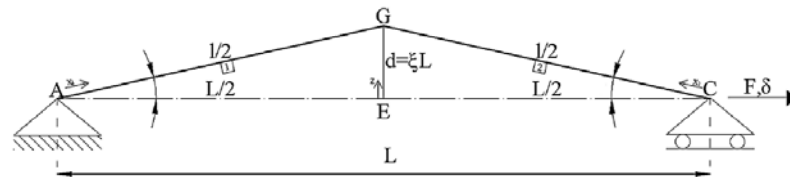
95 Previous work conducted on the Crescent-Shaped Braces by Palermo et al. (2015) led to the
 96 derivation of analytical formulations for sizing the device based on a target stiffness and a target
 97 yielding strength. Eqs. (1) and (2) represent a simplified version of the original equations developed
 98 in [8]. Strength and stiffness are initially imposed according to the predefined performance
 99 objectives that to be achieved. The process involves a consideration of the structural and non-
 100 structural responses of the studied system. Equation (1) allows obtaining the arm ratio of these
 101 devices, which is the ratio between the arm of the device d and the diagonal length L (see Figure 3).
 102 This ratio can be assumed as 0.1 for preliminary designs. The arm ratio is subsequently replaced in
 103 Eq. (2) to get the target moment of inertia of the CSB device.

104
$$\xi = \frac{M_{pl}}{F_y \cdot L} \quad (1)$$

105 where $\xi = d / L$ represents the arm ratio of the device, d is the device arm, $M_{pl} = W_{pl} \cdot f_y$ is the
 106 plastic bending resisting moment of the cross section, W_{pl} is the plastic section modulus, f_y is the
 107 yield strength, \bar{F}_y is the target yield strength, L is the diagonal length (i.e. the line connecting both
 108 extremities of the device).

109
$$J = \frac{L^3 \cdot \bar{K} \cdot \xi^2}{3 \cdot E \cdot \cos^2 \theta} \quad (2)$$

110 where J represents the cross-section inertia, \bar{K} is the target initial lateral stiffness, E is the
 111 modulus of elasticity of the steel section, θ is the angle formed between the applied force and the
 112 device diagonal (i.e. $\theta = 0$).



114
115 Figure 3. The geometric configuration of the studied device. Adopted from [8]

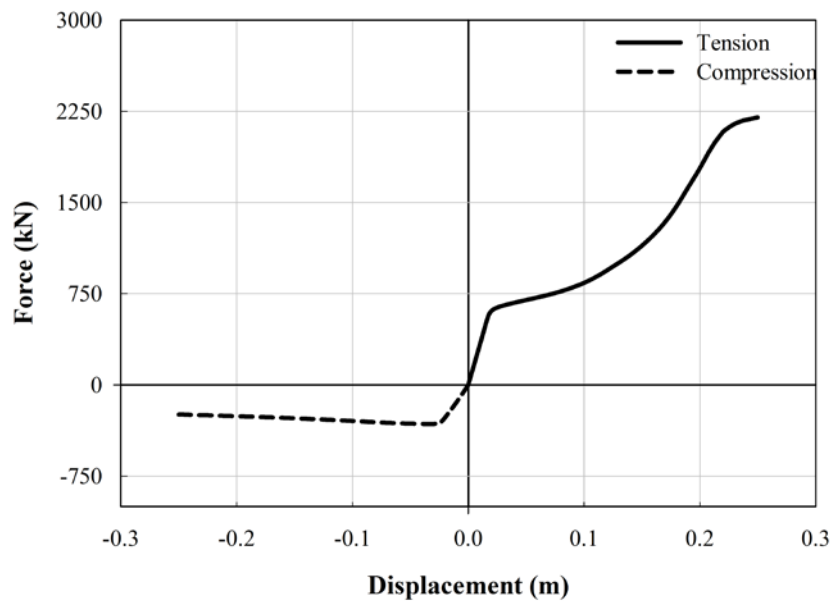
116

117 **2.3 Mechanical behavior of the CSB**

118 The post-yielding behavior of a random CSB device has been numerically studied using the
119 fiber-based software ‘SeismoStruct V.7.0.6’, which considers both geometric nonlinearities and
120 material inelasticity. First, a sample of the bracing device ‘HEB200 European profile’ was subjected
121 to a monotonic rising tension load. The result of the numerical analysis is displayed in Figure 4 (the
122 solid segment of the curve). At the beginning, the CSB responds in flexure, acting linearly until first
123 yielding is reached at the knee section. Then, the device encounters a plastic behavior due to the
124 spread of plasticity (pseudo-horizontal part). This is followed by a second remarkable hardening
125 behavior as the device’s arm d decreases. At this stage, the device mainly reacts through its axial
126 stiffness capacity, like a conventional brace or a truss in a tensile layout.

127 The same specimen was subjected to a monotonically increasing compressive loading. Figure
128 4 (the dotted segment of the curve) is a graphical representation of the constitutive law of the device
129 in compression. It is very important to note that unlike traditional concentric braces, the CSB
130 device does not suffer from sudden Eulerian in-plane buckling when exposed to a compressive
131 force, and this is due to its unique shape. Regarding the out-of-plane buckling, the appropriate
132 selection of the cross section is highly effective in preventing such a problem [8] (e.g. choosing
133 balanced inertias along weak and strong axes). Another solution is to include longitudinal ribs in
134 correspondence to the neutral axis fiber.

135



136

137

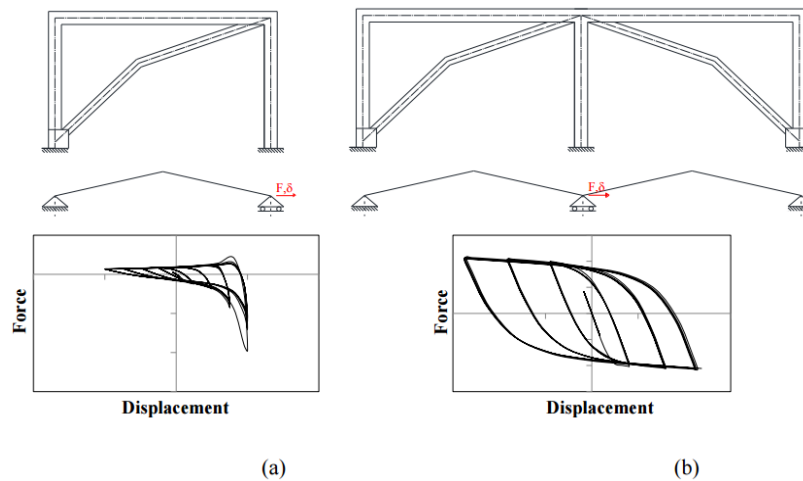
138 Figure 4. Monotonic behavior of a single CSB in tension and compression

139

140 The hysteretic behavior of the CSB is that of typical steel bracings given that the device is
141 nothing more than a steel member having a curved configuration. The numerical studies conducted
142 on the device has demonstrated a good hysteretic response [8]. The simulated hysteretic responses
143 have been also confirmed by experimental tests conducted by some of the authors (the test results
144 will be available soon [10]) and by other researchers [11].

145 The hysteretic force-displacement response of the single CSB device is strongly asymmetric
146 due to the non-linear geometrical effects [8][10]: significant hardening response under lateral loads
147 inducing tension in the brace, and softening response under lateral loads inducing compression in
148 the braces (Figure 5a). On the contrary, when two CSB devices inserted in a two-span frame
149 structure, the overall behavior becomes symmetric given that one works in compression while the
150 other one works in tension (Figure 5b).

151



152
 153 Figure 5. (a) A bilinear CSB device inserted in a frame and its asymmetric force-displacement
 154 response; (b) two mirrored disposed bilinear CSB devices inserted in two frames and their
 155 symmetric force-displacement response. Adopted from[10].
 156

157 3 METHOD: PERFORMANCE-BASED DESIGN OF A MULTI-STOREY SHEAR-TYPE 158 FRAME EQUIPPED WITH CSB DEVICES

159 The design philosophy behind the use of CSBs as enhanced bracings is grounded on the
 160 concept of actively designing a structure behaving according to a so called ‘‘Building–Target
 161 Capacity (B–TC) curve’’ that is then translated into a ‘‘Building–Actual Capacity (B–AC)
 162 curve’’[4]. The B–TC curve is the graphical representation of the idealized seismic behavior of the
 163 building that we expect to achieve by imposing preselected multiple performance objectives, while
 164 the B–AC curve is the graphical representation of the effective seismic behavior of the building,
 165 once all structural members are designed. The use of CSBs at all storey levels is the design strategy
 166 here adopted to achieve the performance design objectives.

167 Given that CSBs can be used in different configurations, several design strategies can be
 168 identified to achieve the desired performance objectives. In the literature, the behavior of an SDOF
 169 steel structure equipped with this device has been investigated [4]. In this section, we propose a
 170 general procedure for the seismic design of multi-storey shear-type frame structures equipped with
 171 Crescent-Shaped Braces (CSB). The proposed method can be used to design or strengthen
 172 structures that do not satisfy particular performance objectives. The design method proposed in the
 173 study involves: (i) designing (sizing) the CSB devices in the elastic field; (ii) verifying the behavior
 174 of the braces within the global system in the plastic field.

175 (i) Designing the CSB devices is done with reference to the performance point corresponding
 176 to the earthquake level *occasional* (EQ2) and the performance level *fully operational* (IO) (Figure
 177 1). This point belongs to the *Essential Objective* performance line, not the ordinary *Basic Objective*
 178 performance line. The reason to choose a high seismic demand is to show the capability of the
 179 braces in achieving a predefined performance level. The sizing method comprises 6 steps. In the first
 180 step, an initial global stiffness matrix for the controlled structure (i.e. structure equipped with
 181 braces) is imposed based on certain criteria, which are described in section 4. The global stiffness
 182 matrix is refined as more iterations are executed. In the second step, a modal analysis for the system
 183 is performed. The building’s drift obtained from the modal analysis is compared to the design drift
 184 that is set according to the desired performance point (i.e. EQ2-IO). The global stiffness matrix is
 185 continuously modified through several iterations until the structure’s drift meets the target drift.
 186 Once the actual drift matches the design drift, we move to step four and we compute the stiffness of
 187 the CSB bracing system. This is done by subtracting the stiffness matrix of the naked structure from
 188 the global stiffness matrix. In step five, the structural configuration (i.e. position and number of
 189 braces) of the CSB system is defined and hence the stiffness of each brace is computed. Finally, by

190 knowing the stiffness of each device, the moment of inertia and the arm of the devices are evaluated
191 in step 6, and this allows choosing a cross-section for the device from a wide range of cross-
192 sections that satisfy the inertia demand. Once the cross-section is known, the post-yielding behavior
193 of the brace is obtained by means of a static nonlinear pushover analysis using the fiber-based FEM
194 software “SeismoStruct V.7.0.6”. SeismoStruct considers the geometric nonlinearity of the model
195 based on the corotational formula [12], and the material nonlinearity in accordance to Menegotto
196 Pinto law, with adequate focus on the isotropic hardening as given in [13]. The stiffness of the
197 device is computed at each step of analysis, and then updated automatically in the following
198 analysis step. Generally, the post yielding behavior of the device is greatly affected by its section
199 profile; therefore, different section profiles must be compared and the one that conforms most to the
200 predefined performance is chosen.

201 (ii) The behavior of the CSB system within the global system is obtained by means of
202 nonlinear static pushover (PO) and dynamic time-history (TH) analyses using the FEM software
203 SAP2000 [14]. The behavior of the equipped structure is verified against the performance points
204 ‘EQ3-O’ and ‘EQ4-LS’ shown in Figure 1. The CSB devices are introduced in the model as multi
205 linear links (NL) by importing the force-displacement curves (backbone curves) of the braces
206 obtained from SeismoStruct software. Using the backbone curves of the braces, SAP2000 updates
207 the stiffness of the device at each analysis step according to the displacement exhibited by the
208 device. The force-displacement curves obtained from SeismoStruct are calibrated in order to
209 account for the structural configuration (inclination) of the devices in the structure. Moreover, the
210 kinematic hysteresis model, which is the default hysteresis model for all metal materials in the
211 program, is considered in the analysis as it is very appropriate for ductile materials. The above
212 mentioned implies that the actual nonlinear stiffness of each device is effectively considered in the
213 analysis. The nonlinearity of the structure is considered using concentrated plastic hinges. The
214 results of both PO and TH analyses are plotted together in order to verify the analysis performed.
215 Finally, the nonlinear pushover curve (i.e. capacity curve) is compared with the predefined
216 performance curve, according to which the devices were initially designed, to check if the target
217 performances are met. Although the nonlinear behavior of the structure equipped with the CSB
218 braces is not designed for ‘automatic’, previous studies suggested that the system would perform in
219 a good way with respect to severe earthquakes [4][15][16][17]. This is mainly due to the shape of
220 the brace (the peculiar mechanical behavior) (Figure 2) and to its hysteretic dissipation properties. In
221 the following section, we introduce the first part of the methodology (i.e. the design of the CSB
222 system), and in section 5 we cover the second part by means of a case study (i.e. the post yielding
223 verification of the braces within the global system).

224

225 4 DESIGN OF THE CSB SYSTEM

226 The dimensioning procedure of the braces is illustrated in Figure 6. The purpose of this
227 design procedure is to obtain a target lateral stiffness for the single CSB device. The stiffness output
228 is then used in the previously delivered design formulas (Eqs. (1) and (2)) to get the inertia demand of
229 the brace. Once securing the moment of inertia, the cross-section profile of the device can be
230 selected from a broad range of cross-sections. In the following, the design procedure of the CSB is
231 described in all details.

232

233

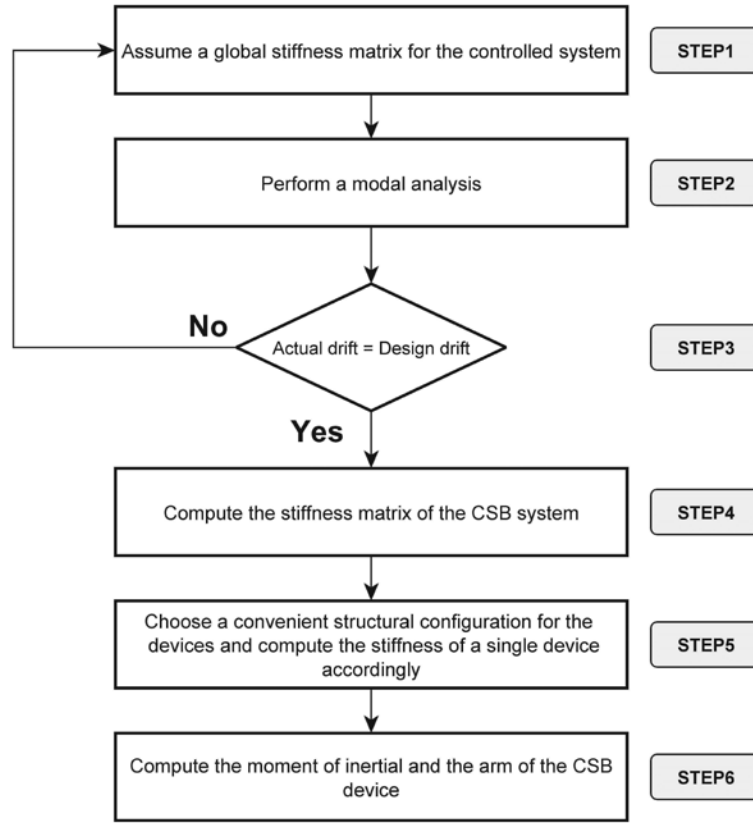


Figure 6. Flowchart of the CSB design scheme

4.1 Step 1: Global stiffness matrix

The global stiffness matrix defines the rigidity of the controlled system. This matrix is determined by summing (as they act in parallel) the stiffness matrices of the bare structure and the bracing system.

$$[K^*] = [K] + [K_b] = \begin{pmatrix} k_1^* + k_2^* & -k_2^* & & & & \\ -k_2^* & k_2^* + k_3^* & \ddots & & & \\ & \ddots & \ddots & & & \\ & & & -k_{N-1}^* & & \\ & & & -k_{N-1}^* & k_{N-1}^* + k_N^* & -k_N^* \\ & & & & -k_N^* & k_N^* \end{pmatrix} \quad (3)$$

where $[K^*]$ denotes the stiffness matrix of the controlled system, k_1^* , k_2^* , ..., k_N^* represent the stiffness terms of the controlled system at the different storey levels. These stiffness terms are mathematically represented as follows:

$$k_i^* = k_i + k_{bi} \quad (4)$$

where k_i^* is the stiffness of the controlled system at storey i , k_i is the stiffness of the uncontrolled system at storey i , k_{bi} is the stiffness of the bracing system at storey i . From the mathematical illustrations above, we see that the global stiffness matrix $[K^*]$ consists of N unknowns, denoted as k_1^* , k_2^* , ..., k_N^* . The number of unknowns, however, can be reduced by

287 where i represents the storey number, u_i is the storey displacement at the i^{th} storey, δ_i denotes the
 288 storey drift between two successive storey levels $i-1$ and i , n is the mode's number, N is
 289 the number of modes.

290

291 4.3 Step 3: Matching the design drifts

292 To achieve the predefined design objective, it is essential that the actual and the design inter-
 293 storey drifts match. Any discrepancy between the two drifts entails adjustment of the global stiffness
 294 matrix. This adjustment is accomplished by adding an increment to the stiffness matrix, as shown in
 295 Eq.(9), and then re-running the modal analysis. This increment is illustrated in Eq. (10). It
 296 is important to note that either of the global stiffness matrices introduced in Eq. (3) and Eq.(6) can be
 297 used in the analysis. Moreover, the designer must verify that the design drift of the structure is less
 298 than its yielding drift. This is because we are conducting a linear analysis, and therefore the elastic
 299 range should not be exceeded.

$$300 \quad k_{i,r+1}^* = k_{i,r}^* + C_{i,r} \quad (9)$$

301

$$302 \quad C_{i,r} = k_{i,r}^* \cdot \frac{\delta_{i,r} - d_{i,r}}{d_{i,r}} \geq 1 \quad (10)$$

303

304 In the above equations, r represents the iteration step, C is the modification coefficient, δ is
 305 the actual drift, d is the design drift, which is obtained from the predefined performance objective.

306

307 4.4 Step 4: Stiffness of the CSB system

308 The target stiffness matrix of the bracing system is acquired by subtracting the stiffness matrix of
 309 the uncontrolled structure from the global stiffness matrix, which is obtained in the final iteration of
 310 step 3. The mathematical equation is given below:

$$311 \quad [K_b] = [K^*] - [K] = \begin{pmatrix} k_{b1} + k_{b2} & -k_{b2} & & & & \\ -k_{b2} & k_{b2} + k_{b3} & \ddots & & & \\ & \ddots & \ddots & & & \\ & & & -k_{b(N-1)} & & \\ & & & -k_{b(N-1)} & k_{b(N-1)} + k_{bN} & -k_{bN} \\ & & & & -k_{bN} & k_{bN} \end{pmatrix} \quad (11)$$

312

313 4.5 Step 5: Stiffness of the single CSB device:

314 In order to obtain the target stiffness of each CSB device, the target stiffness components of
 315 the CSB system $(k_{b1}, k_{b2}, \dots, k_{bN})$ are divided over the total number of devices that exist at the
 316 corresponding storey level, as indicated by Eq. (12). It is the sole responsibility of the professional
 317 designer to assign the number of devices taking into account the architectural constraints in the
 318 building structure.

$$319 \quad K_{CSB,i} = K_{b,i} / N_{CSB,i} \quad (12)$$

320 where $K_{CSB,i}$ represents the stiffness of the single CSB device at the i^{th} storey, $N_{CSB,i}$ is the
 321 number of devices at the i^{th} storey.

322

323 4.6 Step 6: Moment of inertia of the CSB

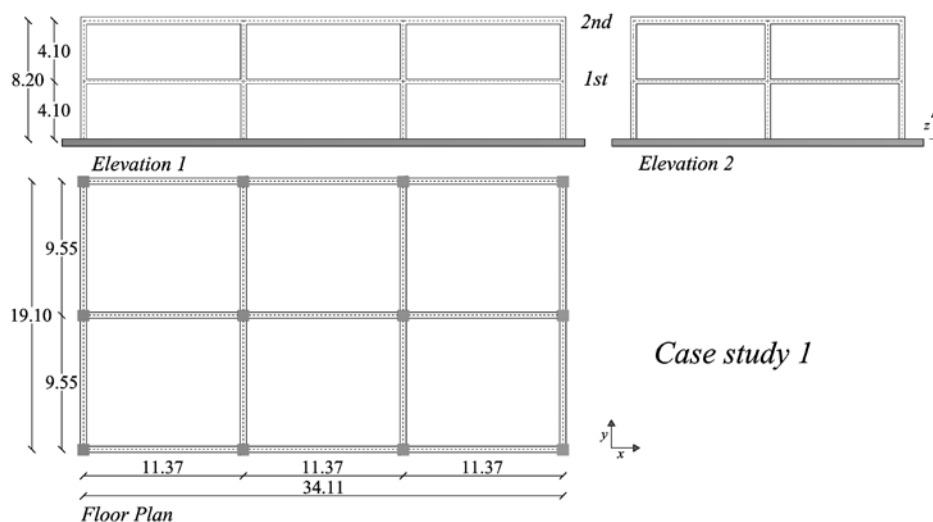
324 At this stage, Eqs. (1) and (2) are used to calculate the moment of inertia of the devices. In
325 these two formulas, \bar{K} is set equal to $K_{CSB,i}$, which is the target stiffness that we seek to
326 achieve, while \bar{F} represents the target yielding strength at which the device goes inelastic. Once
327 securing a moment of inertia for each CSB unit, a cross-section profile for the CSB is chosen from a
328 broad range of cross sections satisfying the target inertia. It is important to note that the cross-
329 section profile choice may dominate the post yielding behavior of the bracing device. This can have
330 a significant impact on the post yielding behavior of the whole structure [8]. Thus, it is necessary to
331 evaluate different cross-section profiles in order to fulfil the inelastic performance objectives
332 (i.e. performance points corresponding to EQ3-O and EQ4-LS shown in Figure 1).
333

334 5 POSTYIELDING VERIFICATION OF THE CSB SYSTEM: CASE STUDIES

335 5.1 The reference structures

336 The first case study structure (CS1) is a new commercial building situated in Gubbio city,
337 Italy. Gubbio is a city located in the far north-eastern area of the Italian province of Perugia, which
338 is in a comparatively high seismic zone. The building was designed according to the Italian seismic
339 standard [18]. Therefore, the building satisfies the operational and the life safety seismic objectives
340 under occasional and rare earthquake levels, respectively. Figure 7 shows the geometry of the building
341 structure. The building is rectangular with dimensions equal to 34.11 m x 19.10 m. It consists of two
342 storey levels with 4.1 m height each. The backbone forming the structure consists of three bays in the
343 y-direction (Elevation 1) and two bays in the x-direction (Elevation 2).

344 The second case study structure (CS2) is an existing elementary school built in 1983. It is
345 located in Bisignano city, Italy, which is also a high seismic zone. As shown in Figure 8, the building
346 structure has a rectangular planar geometry with dimensions equal to 21.39 m x 15.00 m. It is made
347 up of three storey levels with a roof pavilion on the top. The backbone forming the structure
348 consists of four bays in the y-direction and three bays in the x-direction. The mechanical properties
349 of the concrete were determined by the presidency of the council of ministers and the department of
350 civil protection in Italy, who performed ultrasonic and rebound hammer tests on a set of columns
351 and beams. The mechanical and geometrical properties of the concrete elements of both case
352 studies are listed in Table 1.
353



354

355

356

Figure 7. Elevations and plans of the first case study

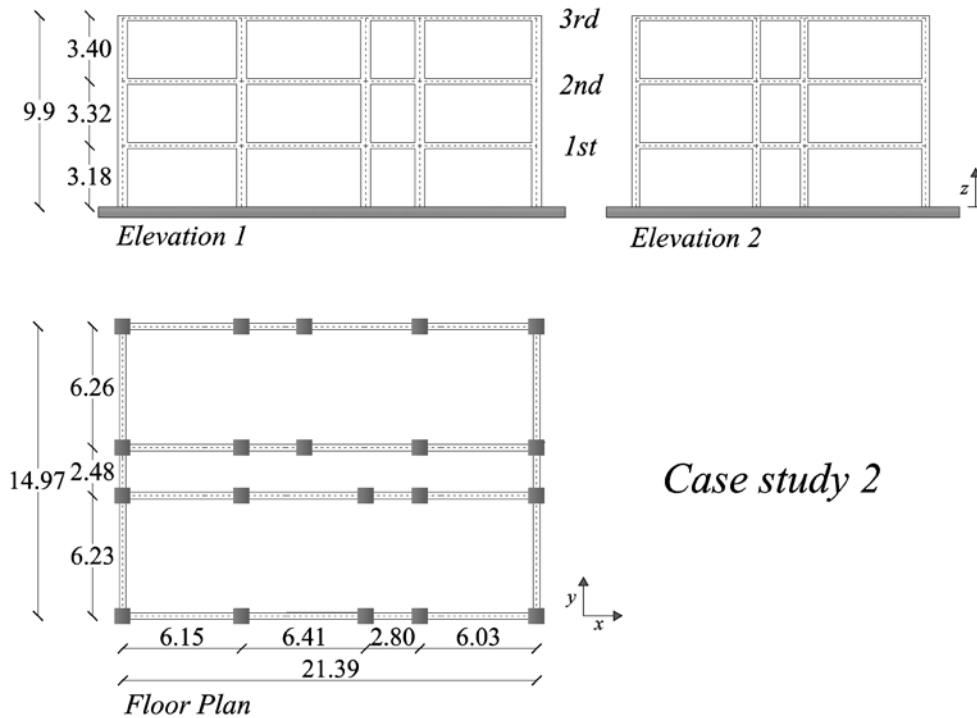


Figure 8. Elevations and plans of the second case study

358
359
360

Table 1 at the end of the paper

362 5.2 Types of analysis

363 Two types of non-linear analysis are performed to verify the performance of the case study
364 structures. A three-dimensional model was built using the commercial software SAP2000 in order to
365 perform the analysis. As recommended by the Italian seismic standard, the loads applied to the
366 structure are: (a) the live loads multiplied by a combination factor (ψ_E); (b) the dead loads without
367 any combination factor. The P- Δ effect was neglected given the small height and the high regularity
368 of the structures. The nonlinear behavior of the frames is modelled using concentrated plastic
369 hinges. Flexural Hinges (type Moment M3) were applied to the beam elements, while flexural
370 hinges (type P-M2-M3) were applied to the columns. The hinge force-deformation relationship,
371 also known as the 'backbone curve', is obtained using the concentrated plasticity model indicated by
372 FEMA 356 [19].

373 After designing the CSB devices as introduced in section 4, the force-displacement curve of
374 each device is obtained using SeismoStruct software by performing a nonlinear static pushover
375 analysis. The Braces are then introduced in the SAP model as multi linear links (NL) by importing
376 the force-displacement curves of the braces. The kinematic hysteresis model is considered in the
377 analysis as it is very appropriate for ductile materials (Figure 9).

378

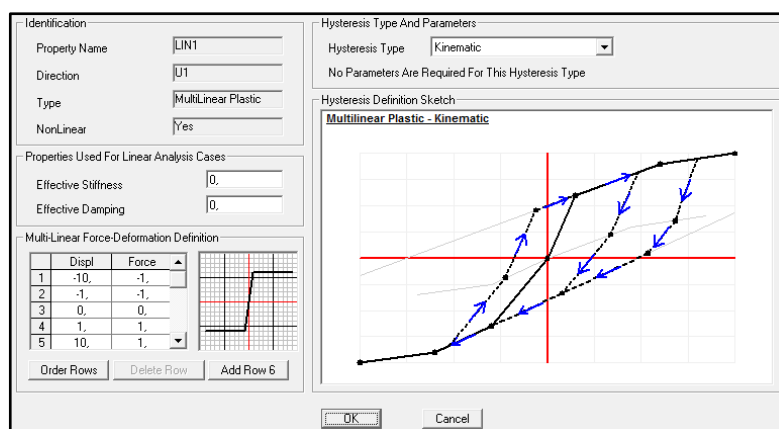


Figure 9. Nonlinear plastic link with kinematic hysteresis type to model the behavior of the CSB in SAP2000.

379

380

381

382

383

384

385

386

387

388

389

390

391

392

393

394

395

396

397

398

399

400

401

402

The first type of analysis is the static pushover analysis, which yields the capacity curve of the structure starting from rest until the failure point [20]. In this analysis, two displacement shapes were applied 'linear' and 'uniform', whose average is considered. The pushover curve was obtained in terms of the base shear and the roof (top) displacement. The second type of analysis is the dynamic time-history analysis, which was performed using the non-linear direct integration method with a damping ratio of 5%. The analysis was conducted by scaling a set of seven accelerograms to the four design values of PGA at the fundamental period of the structure. The ground motion accelerograms needed for the time-history analysis have been obtained using the software *SIMQKE_GR* [21]. The accelerograms are consistent with the design spectra of the structure given by the Italian seismic standard. The Earthquake design levels and the corresponding response spectra parameters are indicated in Table 2. In the table, T_y represents the return period of the design earthquake, PGA is the peak ground acceleration, F_0 is the maximum spectral dynamic amplification, T_c^* is the characteristic period at the beginning of the constant velocity branch of the design spectrum. As shown in the table, the design requirements of the school (CS2) are more stringent than the commercial structure (CS1). The reason is that schools are generally more vulnerable than other types of structures.

Table 2 at the end of the paper

5.3 Structural configurations and local optimization of the CSB devices

403

404

405

406

407

408

409

410

411

412

413

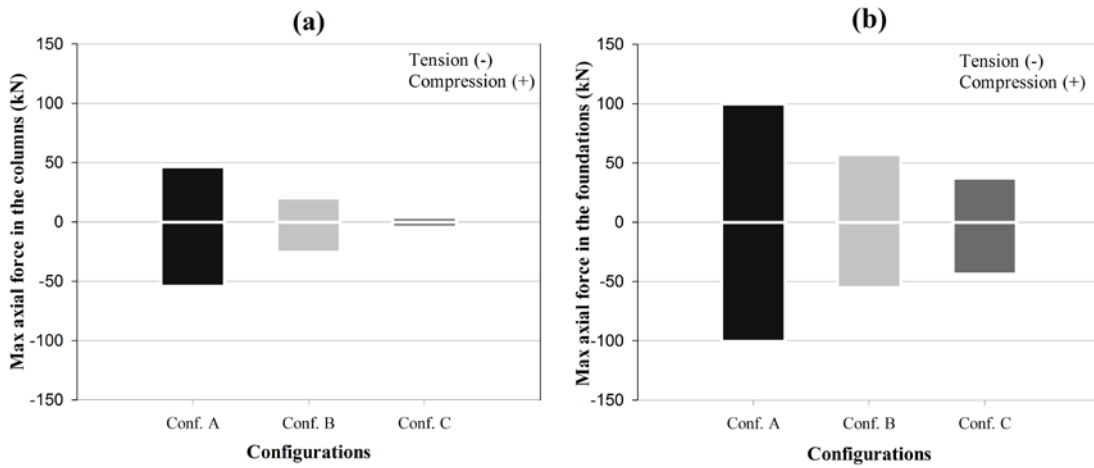
414

415

The structural configuration of the bracing devices defines their effectiveness level. A proper arrangement of the bracing devices in the structure would maximize the lateral resistance capacity while decrease the internal forces in the structural elements. This also leads to a reduction in the devices' cross sections [22]. In addition, high axial force levels can dramatically decrease the moment capacity of columns; therefore, large axial forces should be avoided.

Choosing the right configuration depends on several factors, such as the architectural constraints, the beam span length, and the axial and moment capacities of the columns and foundations. The latter is very important especially if the structure is an existing structure where the structural elements capacities are predetermined. In the design case, on the other hand, the designer can design the columns to stand the additional axial forces coming from the bracing system, and thus this problem can be prevented.

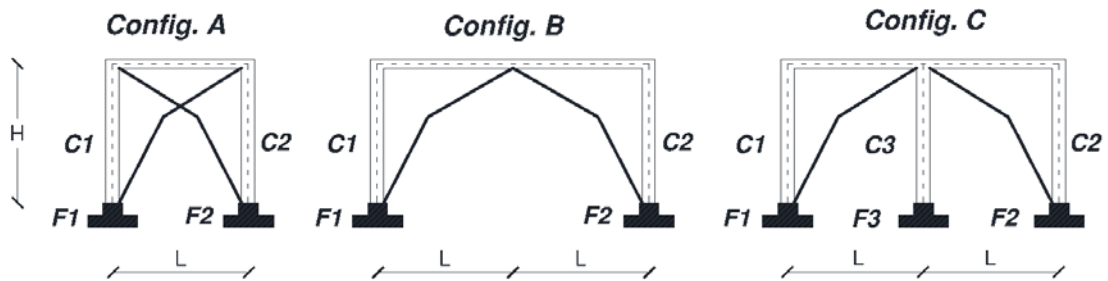
In this section, three possible configurations of the bracing devices (see Figure 10) are investigated by performing a time-history analysis.



416
417

418 Figure 11 shows the results of the time history analysis in terms of the axial force transmitted
 419 into column (C1) and foundation (F1) for each of the configurations. Config. A indicates the highest
 420 axial forces in C1 and F1 compared to the other two configurations, whereas Config. B shows small
 421 axial forces in columns and foundations. The third configuration Config. C induces almost no axial
 422 force in column C1, while it causes the least amount of forces in foundation F1. Among all three
 423 configurations, Config. C is the best configuration regarding the internal stresses in columns and
 424 foundations; however, this comes at the cost of the resistance efficiency. On the other hand,
 425 although Config. A produces the highest amount of forces in the columns and foundations, the
 426 resistance efficiency is very high. Finally, Config. B seems to be less problematic in the
 427 architectural point of view, as it leaves sufficient area in the façade for windows installation;
 428 nevertheless, it is less resistant than the previous two configurations and it causes concentrated
 429 stress in the mid span of the beam.

430

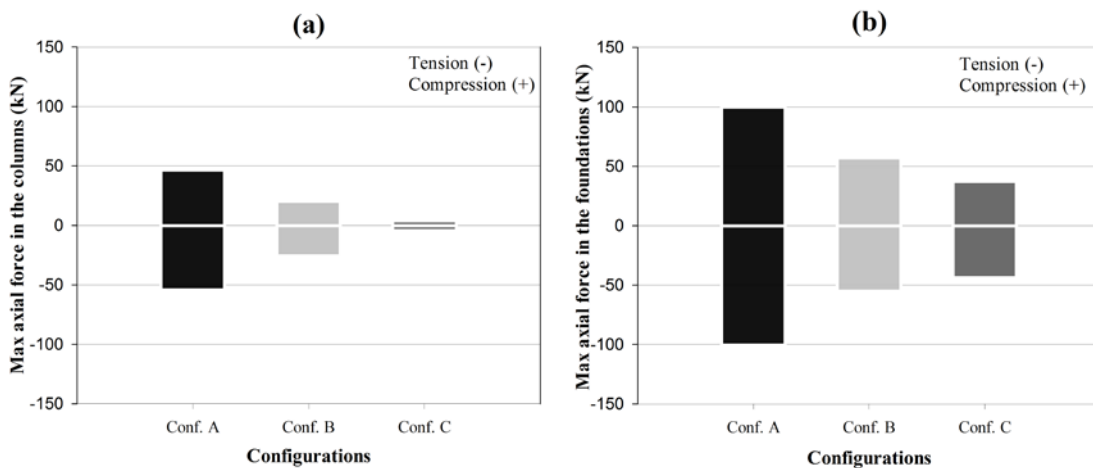


431

432

433

Figure 10. CSB configurations



434

435

436 Figure 11.(a) Maximum axial force in column (C1) for each of the three configurations;(b)
437 maximum axial force in foundation (F1) for each of the three configurations

438

439 5.4 Performance Objectives

440 As we mentioned earlier, the first case study (commercial structure)has been designed in
441 compliance with the Italian seismic standard;therefore,the building satisfies the basic design
442 objectivescorresponding to the two earthquake design levels‘occasional’ and ‘rare’ indicated in
443 Figure 1 and Table 2. The second case study (school), on the other hand, is an existing structure;
444 thus, we need first to verify its performance. This is done byperforming a pushover analysis to
445 capture the base shear level at which the building yields.

446 In this work, higher demands are set to be attained by the structures. The *Essential*
447 *Objectives* specified in Figure 1 are considered instead of the *Basic Objectives*according to which
448 the structures were designed in the first place. The‘Essential Objectives’ require the structure to
449 remain in a fully operational condition under *occasional* earthquake design level (EQ-2), to stay in
450 an operational condition with limited yielding and damages under *rare* earthquake design level
451 (EQ-3), and to have some degree of damage while preventing life losses under *very rare* earthquake
452 design level (EQ-4).

453 The Performance Objectives are usually set depending on the client’s requirements,building’s
454 destination, building’s importance, and building’s typology[15]. A study conducted by Bertero et al.
455 established applicable performance limits on the basis of some structural and non-structural damage
456 criteria, such as structural damage indexes (DM), storey drift indexes (IDI), and rate of
457 deformations (floor velocity, acceleration)[1]. Those performance objectives, however, correspond
458 to the *Basic Objectives* (Figure 1); therefore, they cannot be used in our design because our desire is
459 to fulfil higher requirements. Table 3 reveals the basic objectives corresponding to each of the four
460 earthquake levels, as proposed by Bertero et al. (2002). The table also showstwo proposed sets of
461 performance limits (for the two case studies) belonging to the *EssentialObjectives*. Selecting the
462 new performance limits was done by firstly settingthe inter-storey drift indexcorresponding to EQ-3
463 (PO-3) to a value that insures no structural or nonstructural damage in the structure. The IDI
464 corresponding to PO-3 of the first case study structure is 0.005while it is 0.0045for the second one.
465 The second case study structure was found to yield at a low IDI and this is the reason we set a more
466 stringent performance demand (i.e. IDI=0.0045). Other objective points (PO-1, PO-2, and PO-4)
467 were set proportionally to the corresponding values of PGA at the fundamental period of the
468 structure.

469

470 Table 3at the end of the paper

471

472 5.5 Design of the CSB devicein the x-direction

473 Following the CSB design methodology presented in section 4,Table 4 shows the
474 methodology applied to the two case study structures. The reason of considering two case studies is
475 to show the stability of the design method when applied to structures with different occupancies and
476 different seismic demands. Another reason is to stress that existing structures do not always satisfy
477 the seismic standards. For instance, the second case study structure (existing school) yielded at an
478 inter-storey drift index of 0.0045 (PO-3), which does not comply with the Italian seismic standard
479 that requires the building to yield at a higher drift ratio.

480

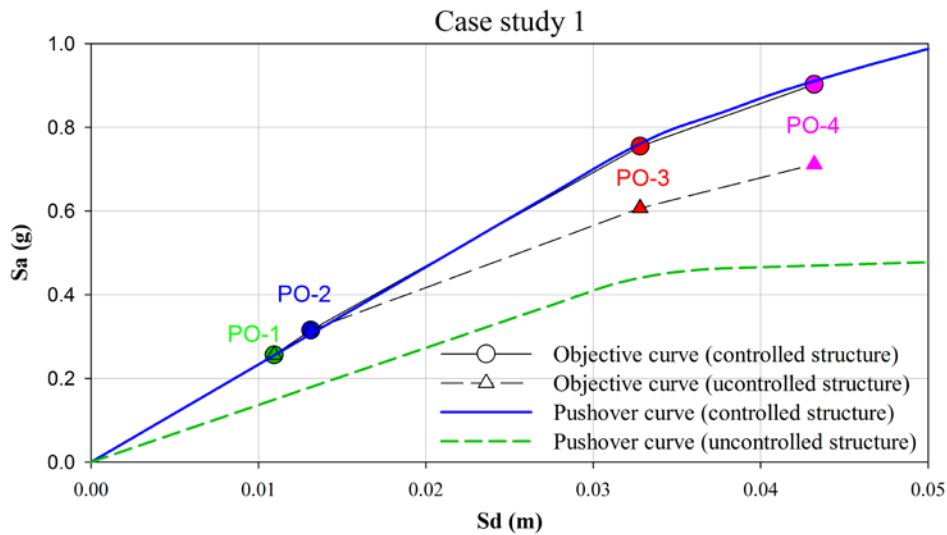
Table 4at the end of the paper

481

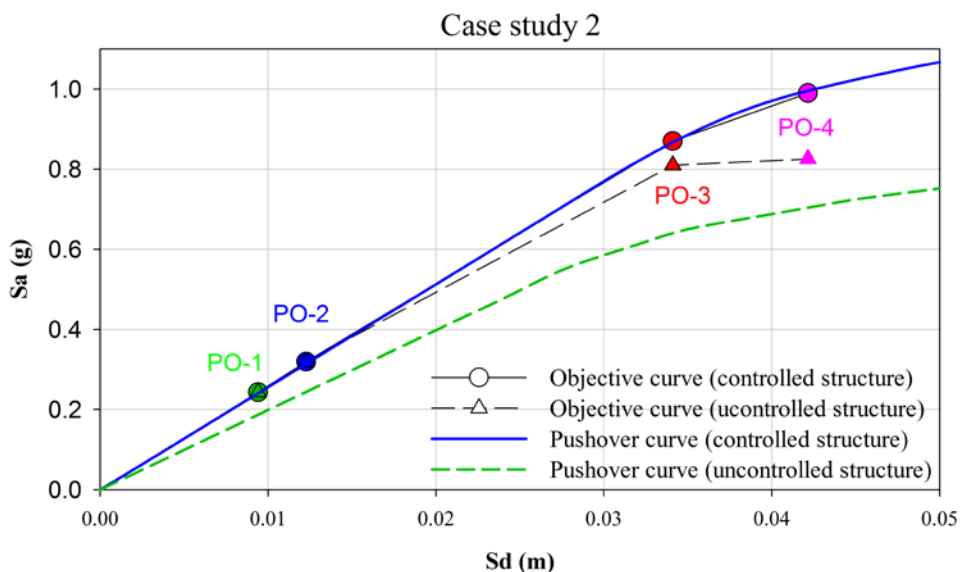
482 **5.6 Numerical verification**

483 In this section, the fulfilment of the pre-defined seismic performance objectives is verified.
 484 This was done through a numerical simulation of the seismic behavior of the two case studies. With
 485 this purpose, a finite element model for each case study has been developed using SAP2000. The fiber-
 486 based software “SeismoStruct V.7.0.6” was used to obtain the constitutive laws of the designed CSB
 487 bracing elements, which were then imported to SAP2000 as non-linear links (NL).

488 First, a non-linear pushover analysis was conducted using two displacement shapes (linear
 489 and uniform), whose average was considered. The base shear and the roof (top) displacement were
 490 used to signify the force and displacement respectively. Figure 12 and Figure 13 show the
 491 capacity spectra of the controlled and uncontrolled structures with their corresponding objective
 492 curves in S_{ad} format for the case studies 1 and 2 respectively. Investigation of the graphs reveals
 493 that for each of the two case studies the capacity spectrum (i.e. pushover curve) of the
 494 *controlled* structure matches the corresponding predefined target curve (i.e. objective curve). On the
 495 other hand, the capacity spectrum of the *uncontrolled* structure was not able to match the
 496 corresponding objective curve.
 497



498
 499 Figure 12. The performance objectives and the results of the pushover analyses in S_{ad} format
 500 of the controlled and uncontrolled structures (Case study 1)

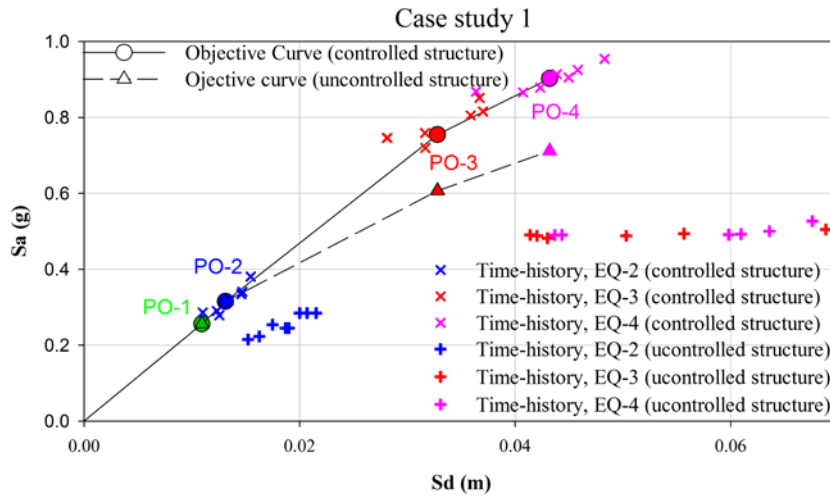


502

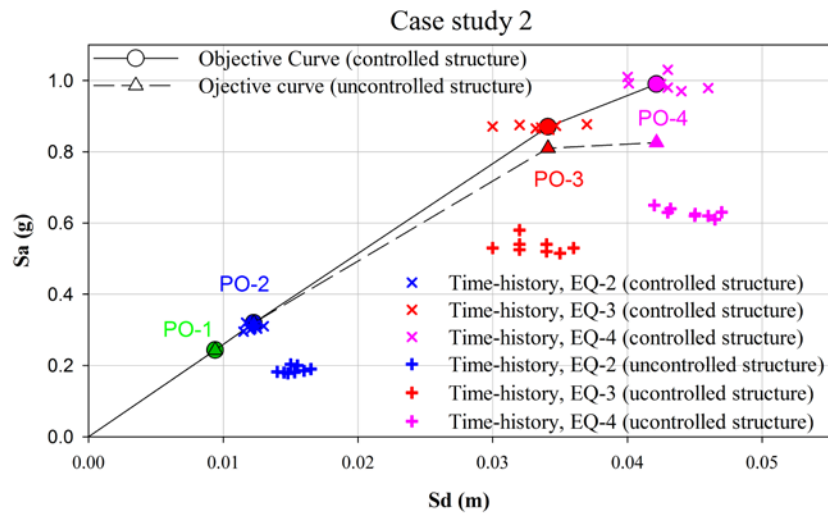
503 Figure 13. The performance objectives and the results of the pushover analyses in S_{ad} format
 504 of the controlled and uncontrolled structures (case study 2)

505 Another type of analysis, nonlinear time-history, was performed to assess the seismic
 506 performance of the structure. Four groups of spectrum-compatible accelerograms were considered
 507 in agreement with the EQ levels reported in Table 2. Each group consists of seven ground motion
 508 records scaled to the PGA of the corresponding EQ level at the fundamental period of the structure.
 509 The results of the time-history analyses for the two case studies are plotted in Figure 14 and Figure
 510 15 respectively, where each point represents the maximum base shear and ultimate displacement of
 511 the corresponding time-history analysis. Investigation of the graph allows observing that the
 512 seismic response of the uncontrolled structure fails to achieve the predefined performances, unlike
 513 the controlled structure whose time-history analyses results show a large agreement with the
 514 prescribed objectives.

515 It is important to note that the nonlinear behavior of the structure equipped with the CSB
 516 braces is not designed for in this study 'automatic'; however, this good behavior is expected due to
 517 the shape of the brace (the peculiar mechanical behavior) (Figure 2) and to its hysteretic dissipation
 518 properties, and this is verified in this study.



519
 520 Figure 14. The performance objectives and the results of the time-history analyses in S_{ad}
 521 format of the controlled and uncontrolled structures (case study 1)



523
 524 Figure 15. The performance objectives and the results of the time-history analyses in S_{ad}
 525 format of the controlled and uncontrolled structures (case study 2)

526 6 CONCLUSION

527 In this paper, a comprehensive procedure for the seismic design of multi-storey frame
528 structures equipped with an energy dissipation device “Crescent Shaped Brace” is proposed. The
529 procedure falls within the Performance-Based Seismic Design (PBSD) approach. The first part of
530 the method is to design the braces in the elastic field with reference to the performance point IO-
531 EQ2. Then, the post yielding behavior of the CSB is determined numerically using the FEM
532 software SeismoStruct. In the second part of the method, the post yielding behavior of the
533 controlled system (i.e. structure equipped with the designed braces) is verified by means of
534 nonlinear pushover and time history analyses.

535 The validity of the method was determined by analyzing two reinforced concrete frame
536 structures equipped with crescent-shaped braces (CSB). First, the performance objectives are chosen.
537 The performance objectives have been expressed in terms of the storey drift index (IDI), which is a
538 measure of the non-structural damage in the structure. Then, the CSB devices have been designed by
539 implementing the proposed design procedure. Static pushover and dynamic time-history analyses
540 were conducted on the case study structures to validate the nonlinear behavior of the CSB within
541 the global system. The analyses performed showed a good behavior of the devices when applied to
542 both case studies although the two structures were of different occupancies and different seismic
543 demands. This confirms the validity of the proposed design approach and the effectiveness of the
544 new hysteretic device in resisting lateral forces regardless of structure’s mechanical properties and
545 the seismic demands.

546 It is important to point out that all prior efforts to design the CSB were majorly based on SDOF
547 structures. The present design procedure is applicable to both SDOF and MDOF shear-type
548 structures. Future research will be aimed at generalizing the method to be applicable to other types of
549 structures.

550 ACKNOWLEDGEMENTS

551 The research leading to these results has received funding from the European Research
552 Council under the Grant Agreement n° ERC_IDEal reSCUE_637842 of the project IDEAL
553 RESCUE— Integrated DEsign and control of Sustainable CommUnities during Emergencies.
554

555 Financial supports of Department of Civil Protection (DPC-RELUIS 2014-2018 Grant –
556 Research line 6 "Seismic isolation and dissipation", WP2: "Energy dissipation", Task 2.6:
557 "Definizione di metodi di progetto, procedure e software dedicati ai sistemi di dissipazione di
558 energia e proposte di normativa sviluppate nell’ambito del presente progetto") is gratefully
559 acknowledged.
560

561 REFERENCES

- 562 [1] R. D. Bertero, V. V. Bertero, Performance-based seismic engineering: the need for a reliable
563 conceptual comprehensive approach. *Earthquake Engineering & Structural Dynamics*,
564 2002; **31** (3): 627-652.
- 565 [2] Özuygur, A. Ruzi, Performance-based Seismic Design of an Irregular Tall Building. *Structures*,
566 2016; **5**: 112-122.
- 567 [3] B. S. Taranath. *Seismic Rehabilitation of Existing Buildings*, Wind and Earthquake Resistant
568 Buildings, CRC Press, 499-584. (2004).
- 569 [4] M. Palermo, I. Ricci, S. Gagliardi, S. Silvestri, T. Trombetti, G. Gasparini, Multi-performance
570 seismic design through an enhanced first-storey isolation system. *Engineering Structures*,
571 2014; **59**: 495-506.

- 572 [5] T. Hoang, K. T. Ducharme, Y. Kim, P. Okumus, Structural impact mitigation of bridge piers
573 using tuned mass damper. *Engineering Structures*, 2016; **112**: 287-294.
- 574 [6] T. K. Datta. *Seismic Control of Structures*, Seismic Analysis of Structures, John Wiley & Sons,
575 Ltd, 369-449. (2010).
- 576 [7] Chopra, K. Anil. *Dynamics of structures: theory and applications to earthquake engineering*,
577 Prentice-Hall, Upper Saddle River, N.J.(2001).
- 578 [8] M. Palermo, S. Silvestri, G. Gasparini, T. Trombetti, Crescent shaped braces for the seismic
579 design of building structures. *Materials and Structures*, 2015; **48** (5): 1485-1502.
- 580 [9] SeismoStruct. "Seismosoft Earthquake Engineering Software Solutions."
- 581 [10] M. Palermo, L. Pieraccini, D. Antoine, S. Silvestri, T. Trombetti, Experimental tests on
582 Crescent Shaped Braces hysteretic devices. *Construction & Building Materials*, (under
583 review).
- 584 [11] H. L. Hsu, H. Halim, Improving seismic performance of framed structures with steel curved
585 dampers. *Engineering Structures*, 2017; **130**: 99-111.
- 586 [12] A. Correia, F. Virtuoso. (2006), "Nonlinear analysis of space frames." Proceedings of the third
587 European conference on computational mechanics: solids, structures and coupled problems
588 in engineering, C. M. S. e. a. (eds), ed., Lisbon.
- 589 [13] F. Filippou, E. Popov, V. Bertero. (1983). "Effects of bond deterioration on hysteretic behavior
590 of reinforced concrete joints." Earthquake Engineering Research Center, University of
591 California, Berkeley.
- 592 [14] I. Computers and Structures. (2015), "SAP2000."
- 593 [15] I. Ricci, S. Gagliardi, G. Gasparini, S. Silvestri, T. Trombetti, M. Palermo. First-Storey
594 Isolation Concept for Multi-Performance Seismic Design of Steel Buildings. *15*
595 *WCEE,2012, LISBOA*.
- 596 [16] O. Kammouh, S. Silvestri, M. Palermo, G. P. Cimellaro. (2016), "Application of Crescent-
597 Shaped Brace passive resisting system as a retrofitting system in existing multi-storey frame
598 structures." 1st International Conference on Natural Hazards & Infrastructure
599 ICONHIC2016, Chania, Greece.
- 600 [17] O. Kammouh, S. Silvestri, M. Palermo, G. P. Cimellaro. (2016), "Application of Crescent-
601 Shaped Brace passive resisting system in multi-storey frame structures." 6th European
602 Conference on Structural Control, Sheffield, England.
- 603 [18] NTC, Norme Tecniche per le Costruzioni, Italian building code, adopted with D.M.
604 14/01/2008, published on S.O. no. 30 G.U. no. 29 04/02/2008. 2008.
- 605 [19] FEMA. (2000). "Seismic Rehabilitation Guidelines."
- 606 [20] T. K. Datta. *Inelastic Seismic Response of Structures*, Seismic Analysis of Structures, John
607 Wiley & Sons, Ltd, 237-274. (2010).
- 608 [21] E. H. Vanmarcke, C. A. Cornell, D. A. Gasparini, S. Hou. (1990), "SIMQKE_GR".
- 609 [22] X. Yu, T. Ji, T. Zheng, Relationships between internal forces, bracing patterns and lateral
610 stiffnesses of a simple frame. *Engineering Structures*, 2015; **89**: 147-161.

611
612

613

Table 1. Mechanical and geometrical properties of the structural elements

Characteristics	CS1 (commercial building)	CS2 (school)
Concrete average cubic strength, R_{ck}	C45/55, $R_{ck}=55$ Mpa	C20/25, $R_{ck}=24.6$ MPa
Steel yield strength, f_y	B540C, $f_y=450$ Mpa	FeB38K, $f_y=375$ Mpa
Modulus of elasticity, E	$E=36000$ Mpa	$E=25150$ Mpa
Columns cross-sections	1 st level 60cmx60cm 2 nd level 50cmx50cm	1 st level 50cmx40cm 2 nd level 50cmx40cm 3 rd level 50cmx40cm
Beams cross-sections	x-direction 50cmx40cm y-direction 50cmx40cm	x-direction 60cmx40cm y-direction 50cmx40cm

614

615

616

617

Table 2. Earthquake design levels with corresponding response spectra parameters for the two case studies

Earthquake design level	Earthquake performance level	T_r [years]		PGA [g]		F_0		T_c^* [s]	
		CS1	CS2	CS1	CS2	CS1	CS2	CS1	CS2
EQ1: frequent	Fully operational-IO	30	45	0.071	0.089	2.39	2.27	0.27	0.29
EQ2: occasional	Damage-O	50	75	0.093	0.116	2.34	2.28	0.27	0.32
EQ3: rare	Life safety-LS	475	712	0.230	0.323	2.39	2.45	0.31	0.38
EQ4: very rare	Near collapse-NC	975	1462	0.293	0.426	1.27	2.49	0.32	0.41

618

619

620

Table 3. Quantification of the Basic and the Essential performance objectives

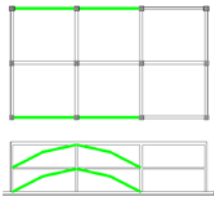
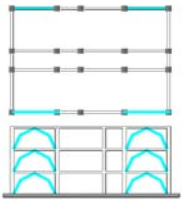
Limit state (Basic objectives)	IDI[1] (Basic objectives)	Limit state (Essential objectives)	IDI (Essential objectives) CS1	IDI (Essential objectives) CS2
EQ1: Fully operational	0.003	EQ1: Fully operational	PO-1 = 0.0015	PO-1 = 0.0013
EQ2: Damage	0.006	EQ2: Fully operational	PO-2 = 0.0020	PO-2 = 0.0018
EQ3: Life safety	0.015	EQ3: Damage	PO-3 = 0.0050	PO-3 = 0.0045
EQ4: Near collapse	0.020	EQ4: Life safety	PO-4 = 0.0067	PO-4 = 0.0055

621

622

Table 4. Application of the proposed design methodology to the two case studies

First case study:	Second case study:
<i>Step 1: Global stiffness matrix</i>	
<ul style="list-style-type: none"> ❖ Mass matrix: $[M] = \begin{pmatrix} m_1 & 0 \\ 0 & m_2 \end{pmatrix} = \begin{pmatrix} 8781.55 & 0 \\ 0 & 7035.165 \end{pmatrix} (kN)$ ❖ Initial stiffness matrix: $[K] = \begin{pmatrix} 338474 + 163230 & -163230 \\ -163230 & 163230 \end{pmatrix} \left(\frac{kN}{m} \right)$ ❖ Initial global stiffness matrix for the first iteration: $[K^*] = \begin{pmatrix} 1 + 0.615 & -0.615 \\ -0.615 & 0.615 \end{pmatrix} \cdot k_1 \left(\frac{kN}{m} \right)$ For the first iteration: $k_1^* = k_1 = 338474$ kN/m	<ul style="list-style-type: none"> ❖ Mass matrix: $[M] = \begin{pmatrix} m_1 & 0 & 0 \\ 0 & m_2 & 0 \\ 0 & 0 & m_3 \end{pmatrix} = \begin{pmatrix} 3799.5 & 0 & 0 \\ 0 & 3470.1 & 0 \\ 0 & 0 & 3153.08 \end{pmatrix} (kN)$ ❖ Initial stiffness matrix: $[K] = \begin{pmatrix} 362800 + 318810 & -318810 & 0 \\ -318810 & 318810 + 189340 & -189340 \\ 0 & -189340 & 189340 \end{pmatrix} \left(\frac{kN}{m} \right)$ ❖ Initial global stiffness matrix for the first iteration: $[K^*] = \begin{pmatrix} 1 + 0.942 & -0.942 & 0 \\ -0.942 & 1.396 & -0.454 \\ 0 & -0.454 & 0.454 \end{pmatrix} \cdot k_1^*$ For the first iteration: $k_1^* = k_1 = 362800$ kN/m
<i>Step 2: Modal analysis (LS response spectrum)</i>	

❖ Inter-storey drifts: $\delta_{01} = 2.63cm$ $\delta_{12} = 3.46cm$	❖ Inter-storey drifts: $\delta_{01} = 2.11cm$ $\delta_{12} = 1.90cm$ $\delta_{12} = 1.84cm$
<i>Step 3: Matching the design drifts</i>	
❖ Design drifts: $\delta_{01,d} = 0.005.h = 0.005 * 410 = 2.05cm$ $\delta_{12,d} = 0.005.h = 0.005 * 410 = 2.05cm$ ❖ Global stiffness matrix at the final iteration: $[K^*] = \begin{pmatrix} 826650 & -312290 \\ -312290 & 312290 \end{pmatrix} \left(\frac{kN}{m}\right)$	❖ Design drifts: $\delta_{01,d} = 0.0045.h = 0.0045 * 318 = 1.43cm$ $\delta_{12,d} = 0.0045 * 332 = 1.49cm$ $\delta_{23,d} = 0.0045 * 340 = 1.53cm$ ❖ Global stiffness matrix at the final iteration: $[K^*] = \begin{pmatrix} 923770 & -401980 & 0 \\ -401980 & 631000 & -229020 \\ 0 & -229020 & 229020 \end{pmatrix} \left(\frac{kN}{m}\right)$
<i>Step 4: Stiffness of the CSB system</i>	
❖ Stiffness matrix of the bracing system: $[K_b] = [K^*] - [K] = \begin{pmatrix} 324950 & -149060 \\ -149060 & 149060 \end{pmatrix} \left(\frac{kN}{m}\right)$ $k_{b1} = 175890 \frac{kN}{m}$ $k_{b2} = 149060 \frac{kN}{m}$	❖ Stiffness matrix of the bracing system: $[K_b] = [K^*] - [K] = \begin{pmatrix} 242160 & -83170 & 0 \\ -83170 & 122850 & -39680 \\ 0 & -39680 & 39680 \end{pmatrix} \left(\frac{kN}{m}\right)$ $k_{b1} = 158990 \frac{kN}{m}$ $k_{b2} = 83170 \frac{kN}{m}$ $k_{b3} = 39680 \frac{kN}{m}$
<i>Step 5: Stiffness of the single CSB device</i>	
❖ Structural configuration of the CSB in the commercial building  $N_{CSB,1} = N_{CSB,2} = 4$ $k_{CSB,1} = \frac{175890}{4} = 43972.5 \frac{kN}{m}$ $k_{CSB,2} = \frac{149060}{4} = 37265 \frac{kN}{m}$	❖ Structural configuration of the CSB in the school building  $N_{CSB,1} = N_{CSB,2} = N_{CSB,3} = 8$ $k_{CSB,1} = \frac{158990}{8} = 19873.7 \frac{kN}{m}$ $k_{CSB,2} = \frac{83170}{8} = 10396.2 \frac{kN}{m}$ $k_{CSB,3} = \frac{39680}{8} = 4960 \frac{kN}{m}$
<i>Step 6: Moment of inertia and cross section profile</i>	
❖ Arm ratio: $\xi = 0.1$ ❖ Moments of inertia: $J_1 = 139684.3 cm^4$ $J_2 = 118377 cm^4$ ❖ Cross sections: CSB_1 : rect. $48cm \times 15cm$ CSB_2 : rect. $45cm \times 15cm$	❖ Arm ratio: $\xi = 0.1$ ❖ Moments of inertia: $J_1 = 5580.3 cm^4$ $J_2 = 3277.8 cm^4$ $J_3 = 1671.5 cm^4$ ❖ Cross sections: CSB_1 : rect. $20cm \times 8.4cm$ CSB_2 : rect. $18cm \times 6.8cm$ CSB_3 : rect. $14cm \times 7.3cm$